

This is the preprint version of the contribution published as:

Luo, J., Luo, Z., Xie, J., Xia, D., Huang, W., **Shao, H.**, Xiang, W., Rohn, J. (2018):
Investigation of shallow geothermal potentials for different types of ground source heat pump
systems (GSHP) of Wuhan city in China
Renew. Energy **118**, 230 - 244

The publisher's version is available at:

<http://dx.doi.org/10.1016/j.renene.2017.11.017>

Investigation of shallow geothermal potentials for different types of ground source heat pump systems (GSHP) of Wuhan city in China

Jin Luo^{a*}, Zequan Luo^a, Jihai Xie^b, Dongsheng Xia^b, Wei Huang^a, Haibin Shao^c, Wei Xiang^a, Joachim Rohn^d

^aFaculty of Engineering, China University of Geosciences (Wuhan), Wuhan 430074, P.R. China

^b Wuhan Geomatic Institute, No.209 Wansongyuan Road, MUA District, Wuhan 430022, P.R. China

^c[UFZ, Leipzig, Germany](#)

^dGeoZentrum Nordbayern, Schlossgarten 5, University of Erlangen-Nürnberg, 91054 Erlangen, Germany

*Corresponding author: Dr. Jin Luo

Telephone: +8602767883044

Fax number: +8602767883507

Email address: jinluo@cug.edu.cn

ABSTRACT

To ensure techno-economically suitable installation of ground source heat pump (GSHP) systems, thermal and hydrogeological properties of the subsoil need to be investigated. In this paper, the geothermal potential for three types of GSHP installations in the urban area of Wuhan city is assessed based on preliminary geological investigations. The potential for shallow geothermal energy is evaluated for surface water heat pump systems (SWHP), groundwater heat pump systems (GWHP) and ground coupled heat exchanger heat pump systems (GCHP). The mapped shallow geothermal potentials provide essential information for the installation of GSHPs and for the management of geothermal resources for Wuhan city. Furthermore, the heat transfer rates for some typical configured BHE are tested by field Thermal Response Tests (TRT). In order to understand the techno-economic feasibility of the GSHPs, different types of the installed systems are measured and

analyzed.

Keywords: Shallow geothermal potentials, Ground source heat pump system (GSHP), Surface water, Groundwater resource, Thermal Response Tests (TRT)

1. Introduction

Geothermal energy has been recognized as an alternative resource for the traditional fuel energy due to the attractive advantages of renewability, cleanness and cost-effectiveness [1]. Nowadays, shallow geothermal technologies are widely used in industrial, commercial and residential buildings for heating and cooling purpose [2]. The shallow geothermal resources are available via surface water, i.e. rivers and lakes, groundwater aquifers and ground soil/rock [3]. In general, the shallow geothermal energy is either explored directly or used by heat pump systems with the coupling of ground heat exchangers [4]. The performance of a geothermal system depends strongly on the site conditions such as geological setting, hydrogeological and geothermal specifications [5]. In order to stimulate the application of shallow geothermal systems for energy generation, geothermal assessments, e.g. geological investigations and geothermal mapping, have been done worldwide in the past decades [6].

Somogyi et al. reviewed the scientific achievements for shallow geothermal systems in six European countries [7]. The environmental effects caused by geothermal systems are introduced in the selected countries. Bertermann et al. mapped the very shallow geothermal potentials of some selected areas in Germany [8]. Thermal conductivity for different soil types and ground temperature distribution were calculated within a depth of 10 m below the ground surface. The obtained dataset were presented on a WebGIS platform for the visualization. The work was a first step for the management and development of shallow geothermal energy systems in the study areas. Casasso and Sethi assessed the shallow geothermal potentials in the province of Cuneo in Italy [9]. The potential for shallow geothermal energy was investigated with different installations for GSHPs including closed-loops and open loops. A geothermal map was presented for identifying the most suitable areas for different installations.

In China, the use of geothermal energy systems has developed rapidly in the past decades. In 2015 an area of about 300 million square meters was used for geothermal heating, and it is expected to reach 500 million square meters in 2020 [10]. Currently, the installed capacity of shallow geothermal energy in China is 27.9×10^9 MWh/yr, and is expected to reach an average growth rate of over 25% till 2020 [11]. In order to encourage a sustainable development of shallow geothermal energy, the evaluation of shallow geothermal potentials of the major capitals of most provinces in China has been conducted [12]. The geothermal resources were assessed based on the initial ground temperature, hydrogeological conditions and thermo-physical properties of the geological materials [13]. The results showed that about 77-1012 million kWh in total can be available each year which are calculated to be equivalent to 9.486 -103 million tons of standard coal [14, 15].

However, the mentioned works in China focus mainly on the evaluation of geothermal resources without paying attention to the specific type of GSHP. Technical and economic feasibility of GSHPs could be largely affected by both, types and site conditions [16]. According to the government's five-year plan, there will be occupied about 11.5 million m² for installations of GSHPs from 2015 till 2020 in Wuhan city [20]. For the sustainable development of shallow geothermal energy, the assessment of geothermal potentials should consider specific GSHP types with small scale geological, hydrogeological and geothermal site conditions [17]. Furthermore, the monitoring of existing GSHPs provides also essential clues for the thermal and economic performance to be expected in the surrounding areas.

In this paper, the shallow geothermal potentials for different GSHP installations in the urban area of Wuhan city are assessed. First, the climate and the geological background of the study area are investigated. Then, the available shallow geothermal energy resources is then assessed for three different GSHP installation types: surface water heat pump (SWHP) system, groundwater heat pump (GWHP) system and ground coupled heat pump (GCHP) system. The mapped geothermal potentials for the urban area within a depth of 120 m of Wuhan city will be presented and heat transport efficiency of typically configured BHE is also determined. Finally, the performance of dozens of installed GWHP and GCHP systems in Wuhan city are investigated.

2. Climate and geological background

2.1 Climate

Wuhan city is the capital of Hubei Province which is located in the middle of China, as shown in Fig. 1. The study area contains a main urban area and nine vicinal districts, covering 8,594 km² area and has 10.6 millions of inhabitants [18]. This area is characterized by a subtropical-humid climate with rather hot summers and cold winters. The annual mean air temperature varies from 15.8 °C to 17.5 °C. During the summer time, the temperature can generally reach up to 37 °C with a record of the highest temperature of 44.5 °C. The winter lasts from December to February with a mean daily temperature of 1-3 °C [19]. Therefore, heating and cooling are both needed for the building's air conditioning with different seasons.

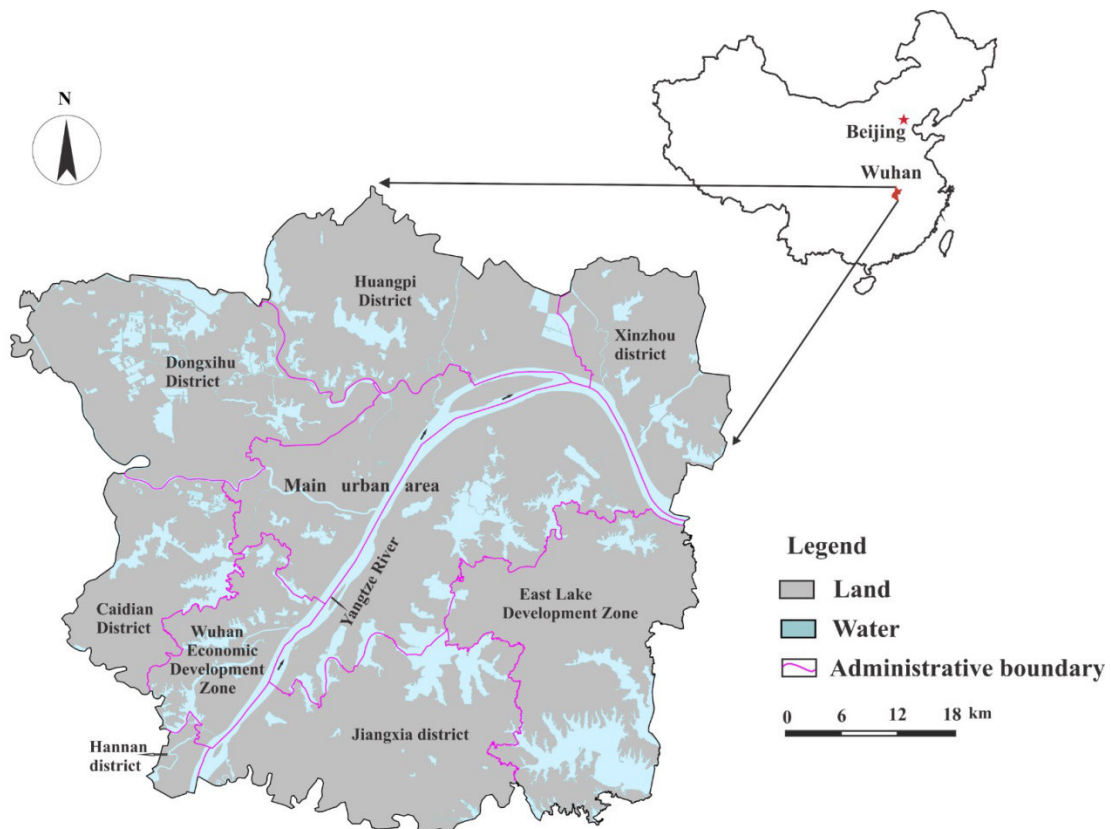


Fig. 1 Map of the urban area of Wuhan city of Hubei province in China. The study area consists of a main urban area and eight sub-urban districts.

Table 1 summarizes the monthly data of temperature, moisture, wind and solar

radiation in the study area [21, 22]. The listed data show that hot weather dominates mainly from June to August. It is observed that the highest temperatures are reached mainly in June, July and August, which is the typical cooling period. The temperature in winter is rather low and varies from 0.4 to 2.3 °C, indicating a heating demand of the local buildings. During the whole year, the humidity remains quite high which means the air has a large heat capacity. All these climatic data provide essential information for the energy consumptions of the buildings in the study area.

Table 1 Monthly climatic parameters in Wuhan city from 2001 to 2009

Month	Jan	Feb	Mar	Apr	May	Jun	Jul	Aug	Sep	Oct	Nov	Dec
Highest temperature (°C)	7.9	10	14.4	21.4	26.4	29.7	32.6	32.5	27.9	22.7	16.5	10.8
Lowest temperature (°C)	0.4	2.4	6.6	12.9	18.2	22.3	25.4	24.9	19.9	13.9	7.6	2.3
Humidity (%)	77	76	78	78	77	80	79	79	78	78	76	74
Wind speed (m/s)	1.8	1.9	2.1	2	1.9	1.9	2.1	1.9	1.8	1.7	1.6	1.7
Average rainfall (mm)	43.4	58.7	95.0	131.1	164.2	225.0	190.3	111.7	79.7	92.0	51.8	26.0
Days for rainfall (d)	9.1	9.5	13.5	13.0	13.2	13.3	11.2	9.0	9.0	9.3	8.0	6.6
Hours for sunshine (h)	104.1	105.4	115.6	151.2	181.8	179.9	232.7	241.2	174.1	161.6	144.3	136.5
Monthly solar radiation (MJ/m ²)	738.7	802.6	994.4	1427.4	1806.9	1939	2842	2673.4	1860.6	1519.9	1187.9	1009.2

2.2 Geological settings

In order to investigate the geological settings, data of 1742 engineering drilling holes and 121 hydraulic observation wells are collected. Fig. 2 depicts the location for these holes and wells in the study area. It is observed that engineering drilling holes are mainly distributed in the main urban area with relatively higher density than the rest 9 sub-urban areas. Thereby, more detailed geological information can be obtained for the main urban area than sub-urban districts. The depths for these drilling holes and wells vary from 50 m to 150 m. All the data cover a period from 2000 to 2016 are collected and provided by Wuhan Geomatic Institute, P. R. China.

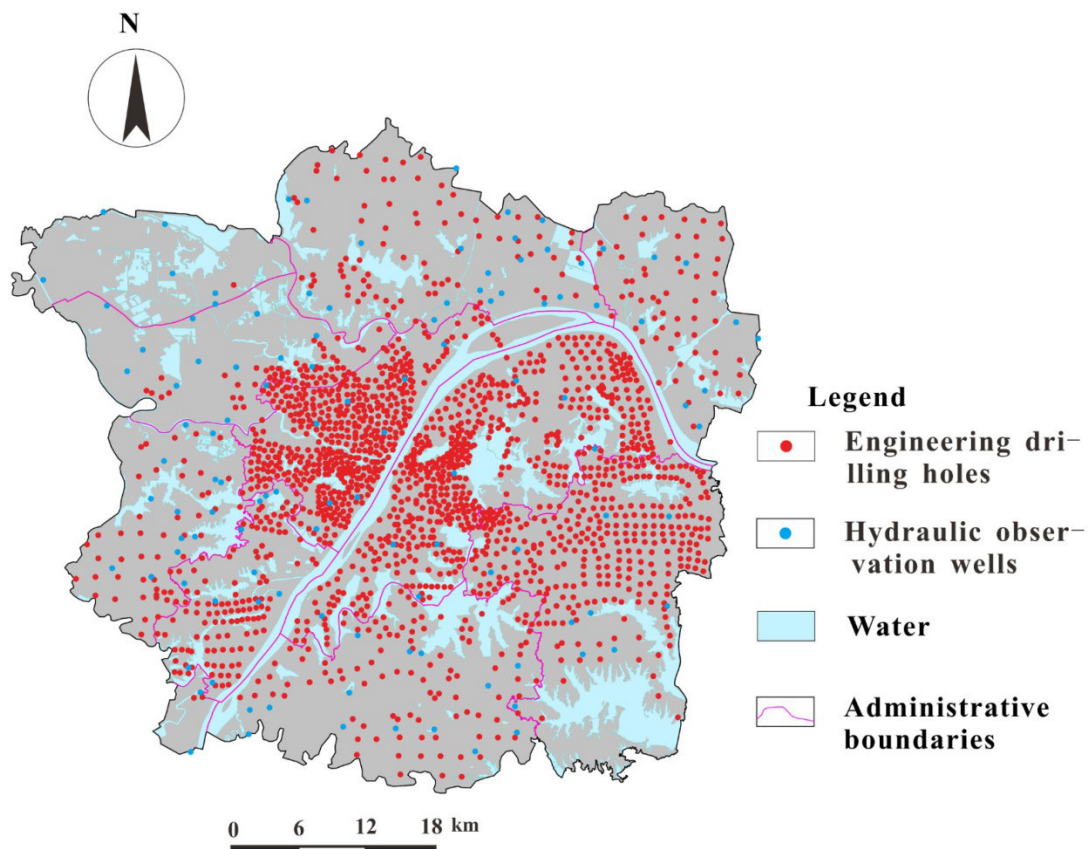


Fig. 2 Engineering drilling holes and hydraulic observation wells used for the geological and hydro-geological investigations

Wuhan city is located in the eastern Jiangnan basin, with Yangtze River and Han River are traversing the city. The geological settings are investigated by collecting data from drilling wells in this area, as shown in Fig. 2, and also by the local

geological map [23, 24]. The subsurface consists mainly of limestone, sandstone and Quaternary river deposits, i.e. gravel, sand, silt and clay. The stratigraphic sequence was investigated in detail. Two categories of geological materials including soils and hard rocks are emphasized for the assessment of the shallow geothermal potential. Fig. 3 shows the geological map with strata and lithology for the study area. Hard rocks formations are mainly distributed in the southern area of Wuhan city and the north part is covered mainly by Quaternary soils. The stratigraphic sequence covers a period from the Silurian to Quaternary period. The lithology of materials includes limestone, sandstones, mud stones and soils.

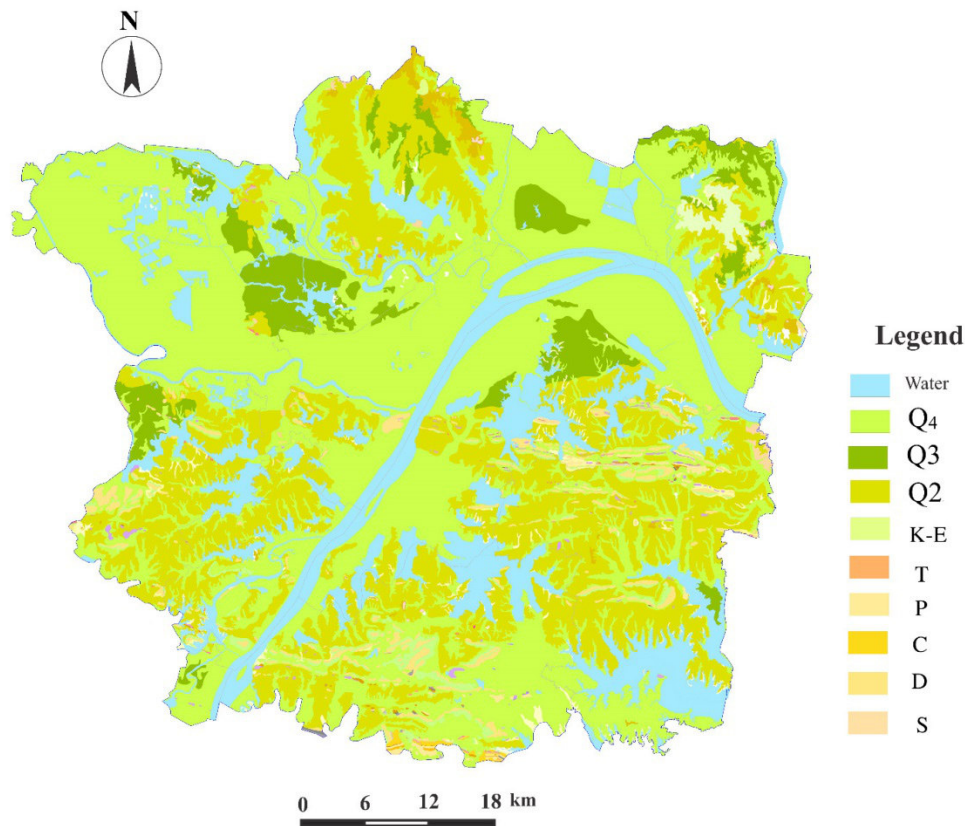


Fig. 3 Geological map for the urban area of Wuhan city. The capital symbols denote different geological ages: S means the Silurian, D is the Devonian, C is the Carbonaceous, P is the Permian, T is the Triassic, K –E is the Cenozoic Era and Q₂₋₃ is the middle Pleistocene and Q₄ is the late Pleistocene.

3. Shallow geothermal potentials

3.1 Surface water resources

To assess shallow geothermal potentials of surface water resources for the installation of SWHP systems, lakes and rivers which are distributed across the study area were investigated. Data was collected from the local water resources bureau of Wuhan city and previous published literature [25]. Table 2 summarizes the information of 33 lakes located in the study area [26]. The volumes of the lakes in the study area vary from $5.42 \times 10^4 \text{ m}^3$ to $8349.68 \times 10^4 \text{ m}^3$. The average depth of these lakes was estimated to be 0.75-3.28 meters, which means temperature of the lakes is largely affected by the air temperature. Furthermore, the temperature of these lakes was also determined. According to the measurements conducted in those selected lakes, the temperature is rather high in summer, as listed in Table 3. The temperature is around one degree lower at the bottom of the lakes than on the surface. The water temperature at the surface and bottom of the lakes was measured using a PT 100 thermometer with a measuring uncertainty of $\pm 0.01 \text{ C}$.

Based on the collected data, the useable thermal energy which can be extracted from lakes was estimated considering the volume of lakes that can be formulated as follows:

$$Q = V \times \rho_f c_f \times \Delta T \quad (1)$$

where V is the volume of pool or lake (m^3), $\rho_f c_f$ is the thermal capacity of water ($\text{MJ}/\text{m}^3\text{K}$), ΔT is the temperature difference ($^\circ\text{C}$). Effects on the biology of the groundwater can be ignored or accepted in case of small-scale system or maximum temperature changes of $\pm 6 \text{ }^\circ\text{C}$ [27].

Considering the lake temperature is rather high in summer and the efficiency for SWHP, the temperature changes from the lakes should lower than the air temperature in summer and higher in winter when assessing the useable geothermal energy. According the temperature measured in the selected lakes in July, the hottest month over a year, the maximum temperature change of the lakes is set $\pm 1.0^\circ\text{C}$. The estimated for seasonal maximum explorable geothermal energy by following Eq. (1) is listed in Table 2.

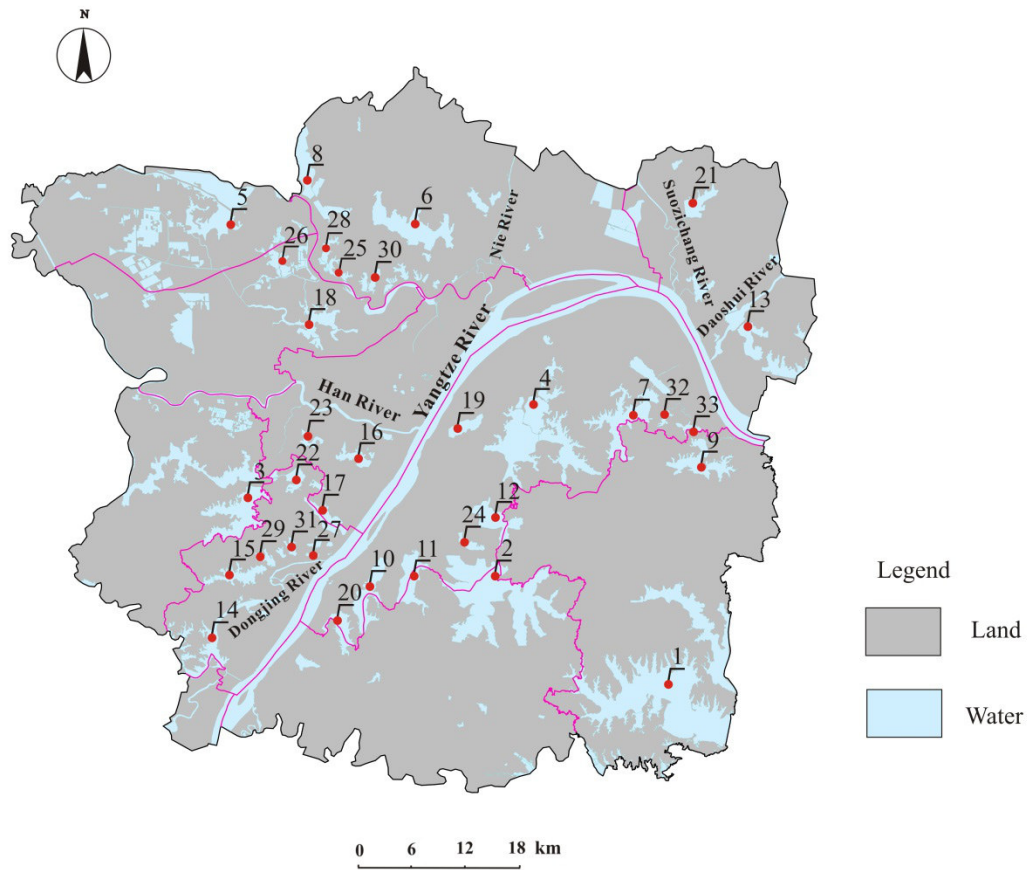


Fig. 4 Major lakes and rivers distributed in the urban area of Wuhan city

Table 2 Summarization of the lakes located and the estimated seasonal explorable energy in the urban area of Wuhan city

Number	Lake name	Area (km ²)	Normal water level (m)	Average depth (m)	Volume (10 ⁴ m ³)	Useable energy (TJ)
1	Niushan Lake	57.2	21.30	1.78	10181.6	427.63
2	Tangxun Lake	52.18	17.63	1.60	8348.8	350.65
3	Houguan Lake	37.30	17.63	1.53	5706.9	239.69
4	East Lake	33.20	19.65	2.73	9063.6	380.67
5	Yaozi Lake	23.40	21.70	1.92	4492.8	188.70
6	Hou Lake	16.32	19.15	1.65	2692.8	113.10
7	Yanxi Lake	14.21	19.13	1.90	2699.9	113.40
8	Tongjia Lake	9.12	22.00	2.2	2006.4	84.27
9	Yandong	9.11	19.15	2.50	2277.5	95.66

10	Lake Qinglin Lake	8.84	17.63	1.5	1326	55.69
11	Huangjia Lake	8.19	17.63	1.70	1392.3	58.48
12	South Lake	7.67	17.63	1.03	790.01	33.18
13	Taojia Lake	4.75	22.00	2.17	1030.75	43.29
14	Guanlian Lake	4.04	18.33	2.2	888.8	37.33
15	Zhushan Lake	3.67	19.00	3.28	1203.76	50.56
16	Moshui Lake	3.64	18.65	2.55	928.2	38.98
17	Nantaizi Lake	3.59	18.63	0.80	287.2	12.06
18	Jinyin Lake	3.29	18.60	2.2	723.8	30.40
19	Sha Lake	3.08	19.15	0.81	249.48	10.48
20	Ye Lake	3.00	17.63	1.4	420	17.64
21	Zhujia Lake	2.52	21.03	1.6	403.2	16.93
22	Sanjiao Lake	2.39	18.63	1.53	365.67	15.36
23	Longyang Lake	1.69	19.15	0.75	126.75	5.32
24	Yezhi Lake	1.62	17.63	1.28	207.36	8.71
25	Majia Lake	1.59	18.56	1.06	168.54	7.08
26	Dugong Lake	1.55	18.60	0.9	139.5	5.86
27	Wangjia Lake	1.40	19.15	2.21	309.4	12.99
28	Renkai Lake	1.34	18.62	1.4	187.6	7.88
29	Lanni Lake	1.21	18.50	2.08	251.68	10.57
30	Panlong Lake	1.13	19.12	1.21	136.73	5.74
31	Tang Lake	1.06	19.00	0.88	93.28	3.92
32	Zuzi Lake	0.67	19.15	1.70	113.9	4.78
33	Qintan Lake	0.60	19.08	1.45	87	3.65

Table 3 The measured temperatures of two selected lakes in Wuhan city

Date (day/ month/ year)	Lake name	Temperature at depth/m	Bottom temperature /°C	Surface temperature /°C	Air temperature/ °C
13/7/2009	Tangxu n lake	1.8	28.94	29.31	32.90
		2.1	28.31	29.19	
		2.5	28.19	29.44	
13/7/2009	East lake	2.3	28.94	29.10	
15/5/2012	East	2.1	23.17	23.64	26.20

	3.5	22.23	23.50
lake	1.4	23.44	23.50

River system is another important surface water resource for SWHPs installation. Temperature of Yangtze River and Han River were monitored during the year 2011-2012 and the monthly mean temperature is plotted in Fig. 5. The data show that temperatures of Yangtze River and Han River change drastically with different seasons. The temperature of Yangtze River varies between 28.2 °C to 10.86 °C for a year period and the Han River shows a more drastic temperature range between 30 °C and 7.69 °C. Parameters include pH-value, electrical conductivity, redbox potential and O₂ content need to be determined in order to assess the suitability for use of the water for heat pumps. Furthermore, the organic substances need also to be investigated for analysis of the water contamination [28].

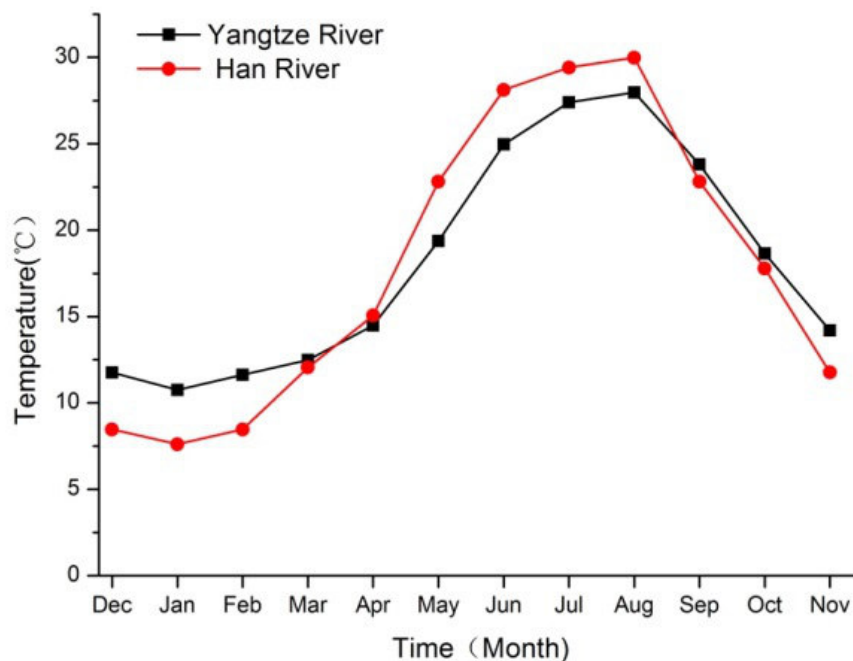


Fig. 5 Measured monthly temperature changes of Yangtze River and Han River between December 2011 and November 2012.

Table 4 The assessed useable geothermal energy for the river systems in the study area

River	Flow rate (m ³ /s)	Useable Energy	
		Summer (GW)	Winter (GW)
Yangtze	33,980	1003	820

Han	1,829	39	20
Dongjing	36.71	0.40	0.77
Nie	12.14	0.13	0.26
Suozichang	46.20	0.51	0.97
Daoshui	22.96	0.25	0.48

The annual flow rate for Yangtze river is 33,980m³/s and Han river is 1,829 m³/s, as shown in Table 4. By considering the outlet temperature from heat pump is 5 °C in winter and 35 °C in summer. The inlet temperature is set by the river's temperature and therefore the maximum useable geothermal energy for hottest month in summer and coldest month in winter is determined. Table 4 lists the maximum energy that can be obtained from both river systems in August and January of Wuhan city. These data provide a reference for the installation capacity of SWHP for the river systems.

3.2 Groundwater as geothermal resource

The evaluation of groundwater as geothermal resource was conducted by considering the open loop GWHP systems in aquifers. For such a system, the water is often pumped from the aquifers. The useable water resource depends on the lithological characteristics, the thickness and the hydraulic properties of the aquifers. In the study area, the groundwater source is mainly used from the Quaternary layers. Main unconfined aquifers are the alluvial deposits of Yangtze and Han River. The thickness varies from few meters to tens of meters in the study area, as it is presented in Fig. 6. Furthermore, confined aquifers such as sandstone layers and limestone are also found in the study area. Due to the low efficiency in well pumping and recharging, the use of confined aquifers as water resource is not encouraged. Therefore, the highly preferred groundwater resources for GWHP systems are mainly the unconfined aquifers.

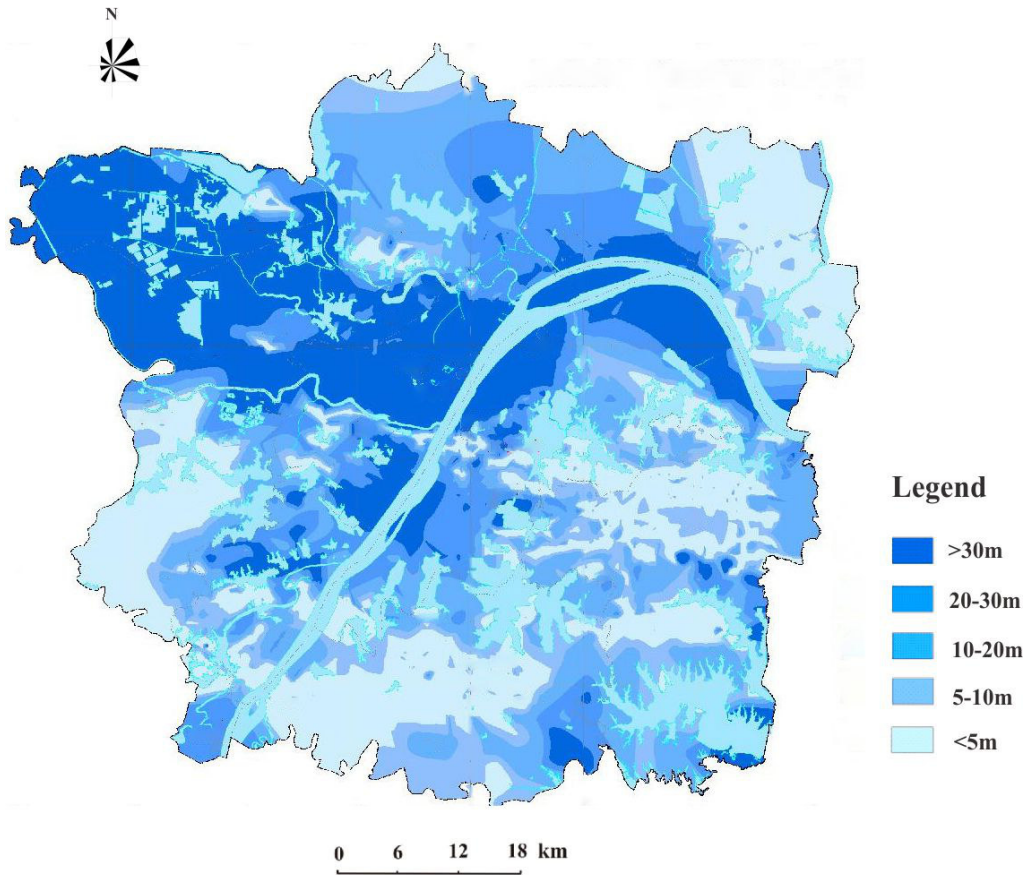


Fig. 6 Thickness of unconfined aquifers in the urban area of Wuhan city

Temperature of the groundwater in the unconfined aquifers was measured and the results show that big seasonal differences. The temperature of the unconfined aquifers can reach up to 20 °C in summer and drops down to 16 °C in winter, with about 4 °C difference over one-year period. The estimation of shallow geothermal potentials for the aquifer systems is conducted by taken into account the pumping rate of the wells. The flow rate of the wells was estimated for both extraction and injection. The hydraulic head drawdown of well is formulated as [29]:

(2)

where S_w is the water head drawdown in the well (m), Q is the pumping rate (m^3/s), KD is Transmissivity (m^2/s), t_{pump} is the time for pumping (s), r_w is the radius of the pumping well (m), S is the storage coefficient (-), C is the coefficient of the quadratic term of the Rorabaugh equation (m^2/s^5). $S=0.2$ is set for unconfined aquifers, t_{pump} is suggested for 200 d [30], r_w is set 0.25 m, $C = 1900 s^2/m^5$ as suggested by Ref [31].

An allowable maximum drawdown for a well can be determined as:

(3)

where α is the a fraction of the saturated thickness (-), b is the thickness of the aquifers (m). A 50% reduction of the saturated thickness ($\alpha=0.5$), was set as suggested by Ref. [30]. The flow rate of injection well is dependent on the hydraulic properties of the aquifers and it is generally lower than the pumping rate. Therefore, the numbers of injection well can be determined based on pumping rate and the specific geological conditions.

By known the flow rate of the wells, the geothermal potential for GWHP installation can then be formulated as:

(4)

where W is the pumping rate of well (m^3/s), $\rho c_f = 4.2 \times 10^6 \text{ J/m}^3\text{K}$ is the thermal capacity of water and $\Delta T = 6^\circ\text{C}$ is set for the temperature difference between injection and abstraction well.

Fig. 7 shows the estimated geothermal potential for GWHP is conducted considering unconfined aquifers in the study area. The mapped shallow geothermal potential can be grouped into four sub-categories. The area with highest explorable geothermal potential distribute mainly at the alluvial deposits of Yangtze River. This area has a relatively thick of unconfined aquifers and with also high hydraulic conductivity. The assessed explorable rate for a single well varies from 233 to 291 kW. The second highly explorable geothermal potential for GWHP installation locates along the deposits of Han River and it is estimated to be 116-145kW. These areas have a similar thickness with the Yangtze deposits but with a lower permeability. Hence, a relatively lower geothermal potential is assessed. The lowest explorable geothermal potential for GWHP is estimated mainly with the unconfined aquifers with a thickness of 5-20 m and it is assessed by 3-20 kW of these areas. The rest are the non-permeable areas which are not recommended for installation of GWHPs.

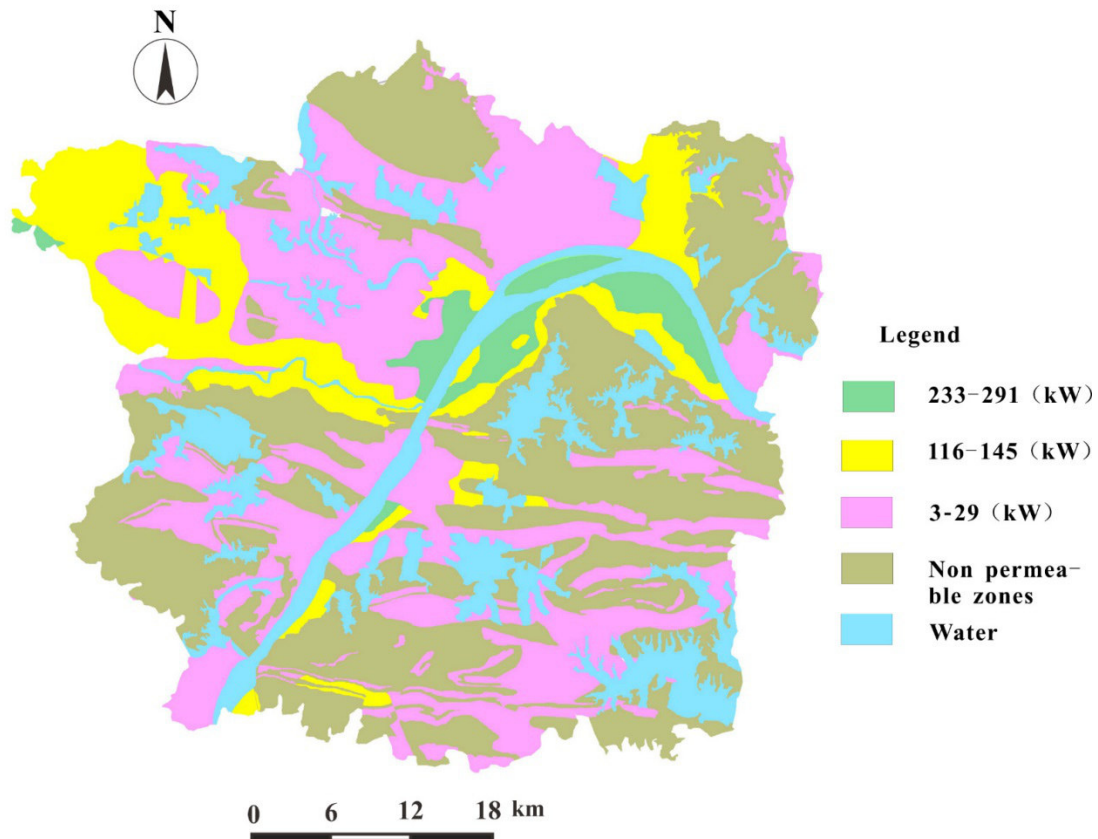


Fig. 7 The evaluated shallow geothermal potentials for ground water heat pump system (GWHP)

3.3 Ground coupled geothermal resources

3.3.1 Determination of the thermal properties

In order to ensure a proper installation of GCHPs, thermal properties of the ground need to be measured. Thermal properties for the geological materials in the study area were determined using the collected drilling samples. In the present work, a portable instrument ISOMET 2114 (Applied Precision Ltd., Staviteľska 1, 83104 Bratislava, Slovakia) was used. A needle probe was applied for determining thermal properties for soft materials such as clay and sand, as shown in Fig. 8a. A steady heating power was applied to the samples and the temperature changes were recorded during the testing process [32]. Thermal properties including thermal conductivity and thermal diffusivity were derived using the records by following heat transfer models (e.g. linear heat source model). On the other hand, thermal properties for the hard materials were measured by adapting a surface probe, as shown in Fig. 8b. The samples were cut and polished to make a flat and smooth surface for the perfect thermal contact with the probe. Around thousand samples were collected and tested for analysis of the

thermo-physical properties of the geological materials.

Determination of thermal conductivity is conducted by the following linear source theory [33] which can be formulated as:

(5)

where λ is the thermal conductivity (W/m·K), q is the heating power (W), T is the temperature °C, Q is the amount of energy (J), t is the time (s), the subscripts 2 and 1 represent the measurements in two different times. Thermal diffusivity can then be derived by temperature variation with time. Thermal diffusivity is the ratio of the [time derivative](#) of [temperature](#) to its [curvature](#), as shown in Eq. (6).

(6)

where T is the temperature (°C), t is the time (s), ∇ is the first order derivativeness, α is the thermal diffusivity (m²/s). Then, volumetric heat capacity can be obtained using thermal conductivity divided by thermal diffusivity [34].



(a) Thermal conductivity measurement for soft soils using a needle probe



(b) Thermal conductivity measurement for hard rocks using a surface probe

Fig. 8 Determination of thermal conductivity for the geological materials of the study area

[Table 5](#) lists the determined thermo-physical properties of the geological materials from Silurian to Quaternary for the collected 874 samples. It is shown clearly that the soft sediment soils have relatively higher water content than the hard rocks. These soils are unconsolidated materials with often large pores and therefore high water contents were observed. In general, thermal conductivity is described by solid matrix, air and water occupied void. Air and water have a relatively lower thermal conductivity than the natural minerals [35]. Therefore, loose materials, i.e. soil, have

generally a lower thermal conductivity than the consolidated materials such as the hard rocks.

Table 5 The determined thermo-physical properties for different lithology in Wuhan city

Geologic Age	No	Lithology	Water content	density	porosity	Thermal capacity	Thermal conductivity
			ω (%)	ρ (g/cm ³)	n (%)	c (10 ³ J/kgK)	λ (W/m·K)
Q4	1	Miscellaneous fill	15-42	1.90	27-60	1.24-1.55	1.13-1.38
	2	Silt	25-83	1.75	30-77	1.48-1.76	1.08-1.33
	3	Clay, silt	20-50	1.89	38-59	1.22-1.51	1.48-1.75
	4	Silt and fine sand	22-46	1.84	40-53	0.98-1.62	1.65-2.22
	5	Sand (fine, middle)	16-61	1.86	34-54	0.96-1.64	1.90-2.47
	6	Sand (middle, coarse)	13-70	1.95	32-56	0.89-1.59	2.30-2.52
	7	gravel	20-63	2.20	40-63	0.81-1.22	2.17-2.49
Q ³	8	Clay, silt	16-30	1.98	38-47	1.13-1.52	1.64-1.89
	9	Clay, gravels	10-34	1.98	30-51	0.94-1.13	1.76-1.96
Q ²	11	Clay, silt	16-29	1.98	36-46	1.06-1.27	1.73-1.97
	12	Clay, gravels	17-26	1.98	29-47	1.25-1.48	1.91-2.04
K-E	13	Sandstone	6-10	2.34	-	1.04-1.28	1.70-2.05
	14	Conglomerate	5.6	2.45	-	0.96-1.09	2.19-2.30
T	15	Limestone	0.2	2.68	-	0.83-0.94	2.65-2.74
	16	Sandstone	6.4	2.44	-	0.76-1.14	2.17-2.52
	17	Shale	8.3	2.43	-	0.73-1.12	2.14-2.37
P	18	Silicolite	0.1	2.73	-	0.71-0.86	2.76-2.88
	19	Limestone	0.4	2.65	-	0.81-0.90	2.48-2.57
C	20	Limestone	0.8	2.68	-	0.83-0.91	2.50-2.64
D	21	Sandstone	0.6	2.60	-	0.74-0.88	2.88-3.07
S	22	Mudstone	8.5	2.47	-	0.88-1.03	2.33-2.48

3.3.2 Temperature measurements

Initial ground temperature is an important parameter for the design and planning of GSHP systems. In this work, the ground temperature was measured within a depth of up to 120 m. A temperature profile in one of the selected locations is presented. [Fig. 9](#)

shows an example for the measured temperature profile at a testing site. It shows that the temperature was seriously affected seasonally by air temperature changes within a depth of 10 m. The ground temperature remains relatively stable with 18.7-20.2 °C through the whole year below such as depth. The geothermal gradient is determined to be 1.5-2.0 °C/100 m with increasing depth.

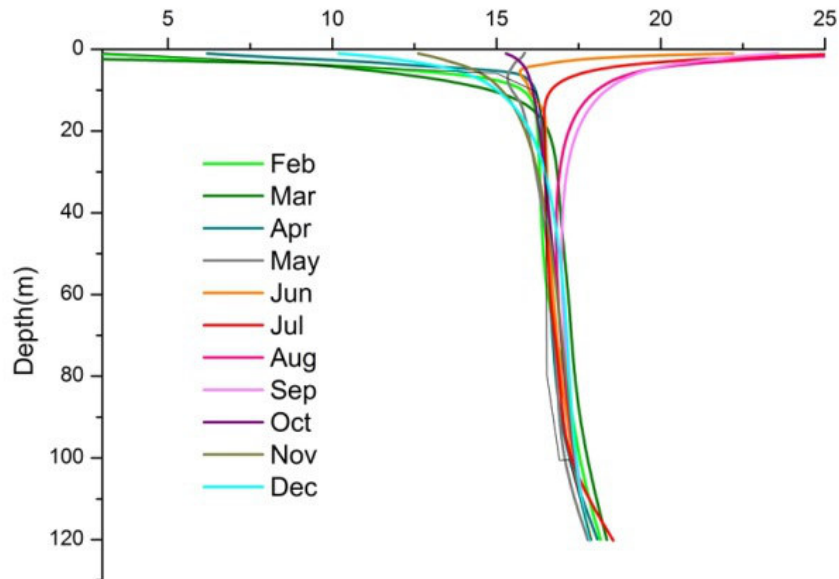


Fig. 9 Temperature profile at a selected testing site in main urban area within a depth of 120 m (Tianfulong Industrial Garden in Caidian District)

Temperature contour lines within a depth of 120 m below the ground surface in the study area were created using a dataset obtained from collected measuring points, as shown in Fig. 2. Fig. 10 shows that the shallow ground temperature varies from 18.2°C to 20.3 °C. The ground temperature in an urban area can be affected by many factors such as buildings, plants and groundwater systems [36]. The mean temperature within a depth of 120 m ranges from 18.3 °C to 20.5 °C in the study area. In the southern region of Wuhan, the temperature ranges between 18.9 °C and 20.5 °C and it varies from 18.5 °C to 19.1 °C in the northern area. The mapped temperature contour line shows a relatively higher temperature in the southern area compared to the northern region. The uneven distribution of the ground temperature can be caused by many factors including lithology, hydrogeological conditions and thermal background of the ground, as shown in Fig. 3 and 6. These data provide a basic understanding of

the initial ground temperature distribution which will be used to assess geothermal potential for GSHP systems.

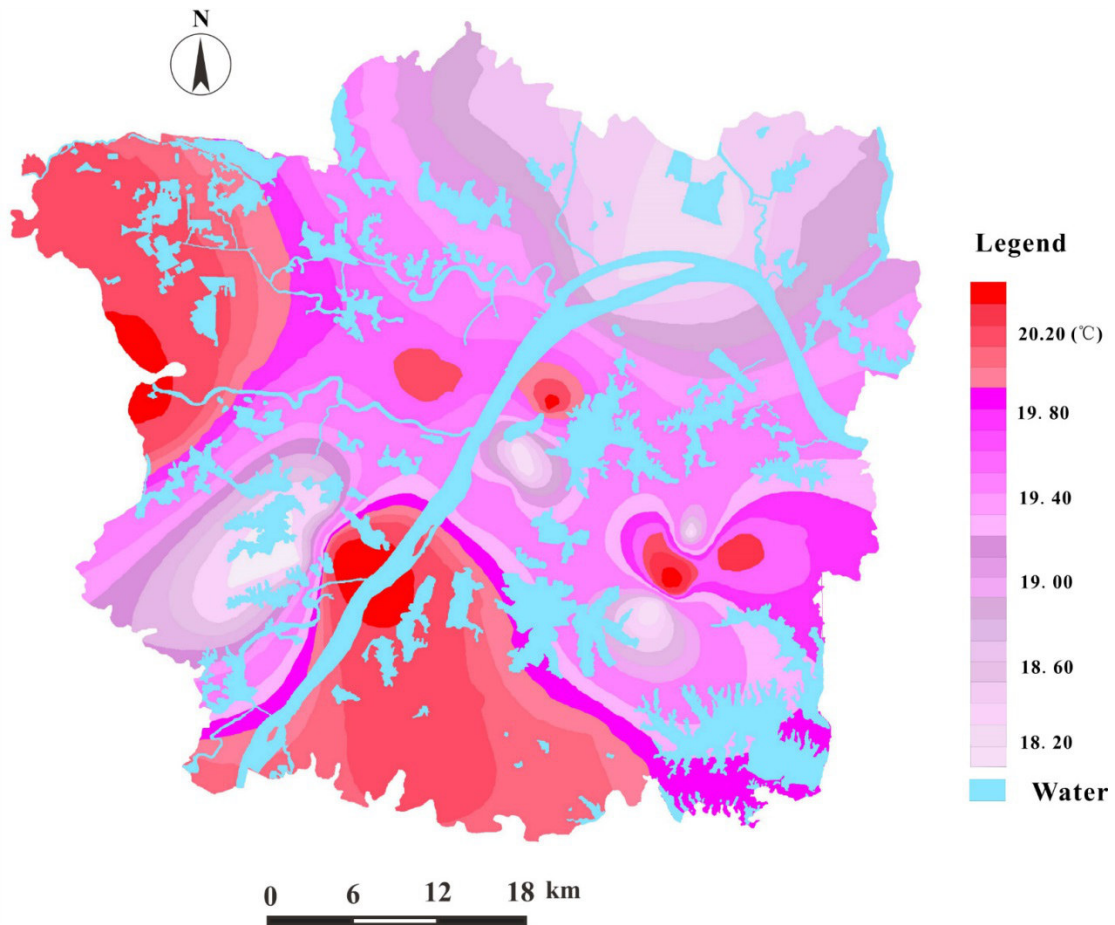


Fig. 10 Mean ground temperature contour line within a depth of 120 m of Wuhan city

Based on the obtained data including geological setting, hydro-geological conditions and thermal properties of the ground materials, shallow geothermal potentials for GSHP are evaluated. The shallow geothermal energy is often explored by using BHE matrix, e.g. layout of 5 m×5 m, and the useable thermal amount can then be assessed considering a seasonal allowable temperature difference and thermal capacity for a unit volume of the ground. The useable thermal amounts can be formulated as follows:

$$(7)$$

$$(8)$$

where Q_{sea} is the seasonal thermal amount (MJ), A is the ground surface area (m^2), Q_+ is the amount of energy extracted from the ground (MJ), Q_- is the amount of energy inject to the ground (MJ), ΔT is the temperature difference ($^{\circ}C$), ρc is the

volumetric thermal capacity ($\text{MJ}/\text{m}^3\cdot\text{K}$) and d_i is the thickness of geological layers (m). In the present work, a total depth of 120 m and temperature difference of $6\text{ }^\circ\text{C}$ is set for assessing the shallow geothermal potential per unit area.

Furthermore, a net energy explorable from the ground is considered due to an unbalanced heat is injected and extracted from the ground with different seasons. The explored net energy is an important parameter indicating a sustainable performance of GSHP system. By considering a 25-year period of GSHP system operation and a mean temperature change of $6\text{ }^\circ\text{C}$, the annual unbalanced net energy is estimated, as it is described in Eq. (5). Fig. 11 shows the mapped the maximum explorable geothermal potential of GCHP for both seasonal and annual net energy amount. It shows the study area can be subdivided into three geothermal areas with different explorable thermal amounts. The mapped highest geothermal potential is 1612.8 MJ, followed by 1526.4 MJ and the lowest area is 1411.2 MJ. The annual net explorable energy is relatively lower than the seasonal explorable energy, with values of 64.0 MJ/yr, 61.1 MJ/yr and 56.4 MJ/yr, respectively. Both parameters are essential to determine an installation capacity with a specific borehole field for GCHPs.

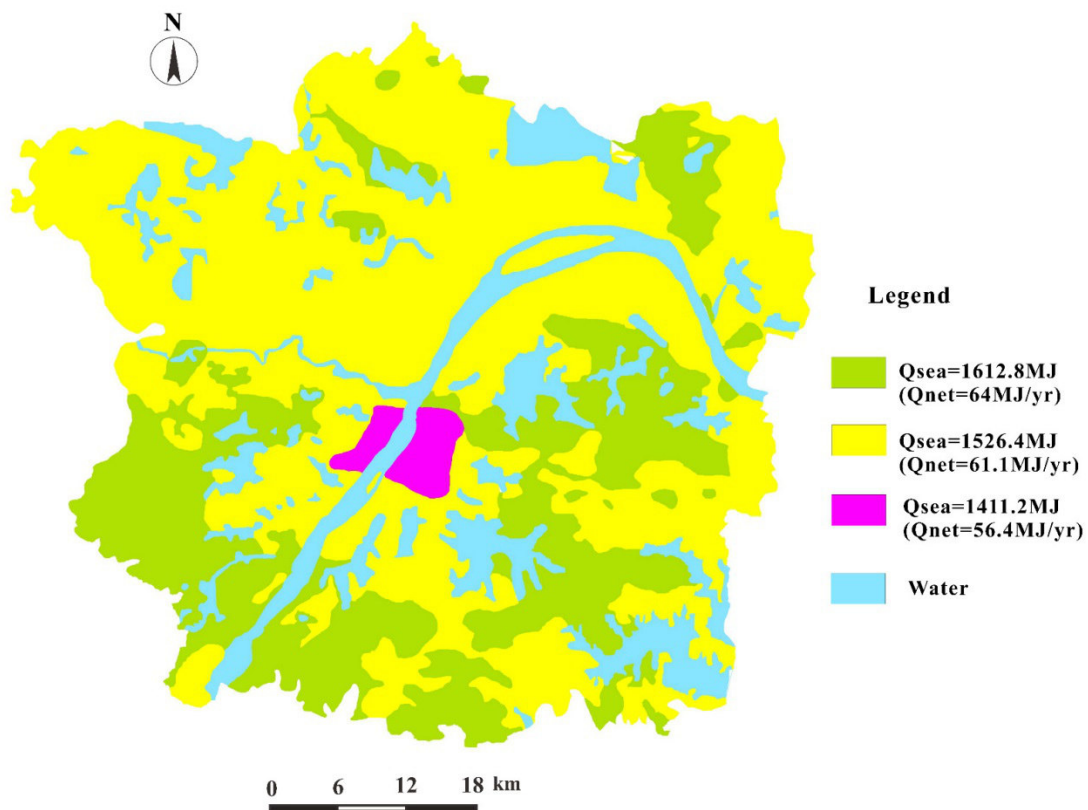


Fig. 11 The evaluated geothermal potentials for ground coupled heat exchanger system (GCHP) per square meters within a depth of 120 m

3.3.3 Thermal Response Test (TRT)

To better understand efficiency for practical exploring geothermal energy by GSHP systems, thermo-physical parameters such as effective thermal conductivity of the ground, heat transfer rate and thermal resistance of borehole heat exchangers (BHE) are of crucial importance. In order to determine thermo-physical parameters in the field, seventeen TRTs were carried out for some selected locations with typical geometric configurations of BHEs.

Undisturbed ground temperature of the ground was first measured by circulating the fluid through the closed loops without power input. Afterwards, a constant heating power is adapted to the heat the carrier fluid and the surrounding ground. Parameters including fluid inlet and outlet temperature and fluid flow rate are continuously recorded during the testing process. Then, the effective thermal conductivity of the ground was determined following the linear source heat transport model. The obtained results are presented in [Table 6](#). Furthermore, the determined specific heat rate for both heating and cooling cases of some typical configured BHEs are presented in [Table 7](#).

During the measuring period of the TRT process, fluid inlet–outlet, flow rate and heat power were continuously recorded. The mean fluid outlet and inlet temperature is used for interpreting thermal properties of the surrounding ground of BHE. In this study, the linear theory was applied to determine the effective thermal conductivity of the ground and the thermal resistance of the borehole [37]. The mean fluid temperature of the heat carrier fluid can be formulated as:

(9)

where, T_f is the fluid temperature ($^{\circ}\text{C}$), T_s is the undisturbed ground temperature ($^{\circ}\text{C}$), q is the power input (W), H is the length of the borehole (m), r_b is the borehole radius (m), t is the time (s), α is the thermal diffusivity (m^2/s) and γ is the Euler constant (0.5772), λ_{eff} is the effective thermal conductivity of the ground (W/mK), R_b is the

thermal resistance of the borehole (mK/W).

By fitting the linear regression between mean fluid temperature versus logarithmic time, Eq. (3) can be shown as:

$$(10)$$

where m is the slope of the linear regression of mean fluid temperature versus logarithmic time.

Borehole thermal resistance, R_b , estimated by the line-source model [38] is given as:

$$(11)$$

Table 6 Collected data from Thermal Response Tests (TRT) implemented in the study area

No.	District	Depth (m)	Lithology	Borehole radius (m)	Type	Initial ground temperature ($^{\circ}C$)	Borehole thermal resistance ($m \cdot ^{\circ}C/W$)	Effective thermal conductivity ($W/m \cdot ^{\circ}C$)
1	MUA	119.5	Silt + Claystone	0.15	Double-U	20.14	0.092	1.81
2	Xinzhou	119.8	Silt + Sandstone	0.15	Double-U	20.18	0.089	2.54
3	Caidian	120.3	Silt + Claystone	0.15	Double-U	20.68	0.121	2.81
4	Hanan	122.7	Silt + Limestone	0.15	Double-U	19.87	0.148	2.39
5	Caidian	120.7	Silt + Sandstone	0.15	Double-U	20.24	0.113	2.30
6	Zhuangkou	99.5	Silt + Sandstone	0.15	Double-U	20.52	0.105	2.74
7	Huangpi	120.5	Silt + Sandstone	0.15	Double-U	20.35	0.115	2.31
8	ELHD	120.8	Silt + Limestone	0.15	Double-U	19.86	0.135	2.01

9	Zhuangkou	94.2	Silt + Sandstone	0.15	Double-U	18.4	-	2.15
10	ELHD	100	Silt + Limestone	0.15	Double-U	18.4	0.142	1.81
11	MUA	70	Silt + Sandstone	0.15	Double-U	18.2	0.142	2.46
12	MUA	100	Silt + Sandstone	0.15	Double-U	18.9	-	2.25
13	ELHD	100	Silt + Sandstone	0.15	Double-U	20.43	0.100	2.94
14	Donxi hu	150	Silt + Sandstone	0.15	Double-U	20.34	-	2.14
15	MUA	100	Silt + Claystone	0.15	Double-U	20.4	0.059	2.10
16	MUA	100	Sand+ limestone	0.15	Double-U	16.5	0.432	3.20
17	MUA	70	Silt + Sandstone	0.15	Double-U	18.6	0.250	2.105

*MUA: main urban area, ELHD: East Lake High-Tech Development Zone

Thermal transfer rate of these BHEs is evaluated by the recorded parameters such as outlet/inlet fluid temperature and fluid flow rate during the testing process. The heat transfer rate can be formulated as:

(12)

where q is the specific thermal exchange rate for the borehole heat exchanger per meter length (W/m), W is the volume of rate of the heat carrier fluid (m^3/s), $\rho_f c_f$ is the heat capacity of the heat carrier fluid ($\text{J}/\text{m}^3 \cdot \text{K}$), T_{outlet} is the outlet fluid temperature for the heat carrier fluid ($^{\circ}\text{C}$), T_{inlet} is the inlet fluid temperature ($^{\circ}\text{C}$), H is the total length of the energy piles (m) [39].

The total lengths of the tested BHEs vary from 70 m to 120 m. Specific heat rate of the BHEs was measured varying from 45.55 W/m to 66.80 W/m, with an mean value of 57.18 W/m. The specific heat rate of BHEs was tested to be changed drastically with differences of ground conditions and geometric configurations of the BHE which are considered as the main factors determining heat transfer of BHEs [40]. Thereby, a mean value can be recommended as a reference for a small-scale GCHP. For a large-scale GCHP system, a TRT is suggested to measure thermal properties of BHEs with specific configurations and ground conditions.

4. Performance of the installed systems

To further understand the technical and economical potentials, the performance of the different types of GSHPs which were installed from 2001 till 2012 was analyzed. Table 8 lists the collected information including locations, covered area for air conditioning, GSHP types and installation year. There are installed in total 58 GSHPs including two types, GWHP and GCHP systems, in the past decade. The size of the installed GSHPs covers a wide range from 1,500-300,000 m². In the earlier period, both GWHP systems and GCHP systems were constructed. However, only GCHP systems were built after the year 2010. In addition, there is only one surface water geothermal system which is in planning to be constructed in the main urban area by Sinopec Co., Ltd, which will cover an area of 1.5 million m² for air conditioning.

Table 8 Ground Source Heat Pump systems Installed in Wuhan city during 2001 to 2012

No	Name	Distri ct	Area (m ²)	Type	Year
1	Wuhan International Expo Center	MUA	420000	GWHP	2001
2	Tianyudi Entertainment Co., Ltd.	MUA	5000	GWHP	2002
3	Lingyun Technology Group	MUA	11000	GWHP	2002
4	Xiangxieli Court	MUA	45000	GWHP	2002

5	Public Security Department Driving School	MUA	6000	GCHP	2002
6	Wuhan Hangda Company	Dong xihu	18000	GWHP	2003
7	Fuxinghuiyu Court	MUA	10000	GWHP	2003
8	Hubei University of Police Canteen	MUA	12000	GWHP	2004
9	Baibuting Garden Court	MUA	12000	GWHP	2004
10	Hubei University Library	MUA	42000	GWHP	2004
11	Wuhan Building Energy Saving Center	MUA	2500	GWHP	2004
12	Qingjiang Garden	MUA	29000	GCHP	2004
13	Wuhan Shabake Entertainment Company	MUA	5000	GWHP	2005
14	Mulan Lake Local Taxation Center	Huan gpi	1500	GCHP	2005
15	Taiyuejing Court	Dong xihu	-	GWHP	2006
16	Wuhan Anju Engineering Development Co., Ltd.	MUA	-	GWHP	2006
17	Dushijingdian Court	MUA	3000	GWHP	2006
18	Wuhan Acrobatic Hall	MUA	6196	GWHP	2006
19	Wuhan Chinese Stone Museum	MUA	-	GCHP	2006
20	Wuhan Art Museum	MUA	-	GWHP	2007
21	Central South Theater	MUA	-	GWHP	2007
22	Hubei Geology and Minerals Bureau	MUA	-	GWHP	2007
23	Hubei Academy of Agricultural Sciences	MUA	-	GWHP	2007
24	Baibuting Supermarket	MUA	-	GWHP	2007
25	Military Economics Academy Library	MUA	36000	GCHP	2007
26	Yulong Court	MUA	-	GCHP	2007
27	Blue Sea Garden Court	Dong xihu	-	GCHP	2007
28	F-world Court	Huan gpi	-	GCHP	2007
29	Ocean Shore Court	MUA	-	GCHP	2007

30	Shouyi Park Court	MUA	-	GCHP	2007
31	Xinrongcun Passenger Station	MUA	11513	GWHP	2008
32	Air Force Radar Academy	MUA	25080	GWHP	2008
33	Sanjinxing Court	MUA	20000	GWHP	2008
34	China Railway SIYUAN Survey and Design Group CO.,LTD	MUA	38986	GWHP	2008
35	Zhengyuan Electrical Buliding	MUA	52300	GWHP	2008
36	Geological Science Research Building	MUA	22000	GWHP	2008
37	Tazihu Lake Sports Center	MUA	-	GWHP	2008
38	Hubei Entry Exit Inspection and Quarantine Bureau	MUA	-	GCHP	2008
39	Dongfeng Court	MUA	45000	GCHP	2008
40	Lanjing Court	MUA	72132	GCHP	2008
41	Jinyuan Court	Jiang xia	120700	GCHP	2009
42	Wuhan Railway Station	MUA	-	GCHP	2008
43	MUA Railway Station	MUA	50000	GCHP	2008
44	Wuhan Pan Group Building	MUA	-	GCHP	2008
45	Fuoguang Lighting Building	MUA	-	GCHP	2008
46	Oriental Hawaii Court	MUA	-	GCHP	2008
47	Swan Lake Villa Building	Caidi an	-	GCHP	2008
48	719 He Tian Club Building	MUA	-	GCHP	2008
49	Landsea International Company	MUA	121608	GCHP	2010
50	Jinhe Family Court	MUA	26000	GCHP	2010
51	Wuhan Municipal Office Building	MUA	12000	GWHP	2010
52	Wuhan Institute of Geological Engineering Building	MUA	4000	GCHP	2010
53	Jingu Court	MUA	13000	GCHP	2011
54	Fingu electronic Building	ELH D	22000	GCHP	2011

55	Hubei University of Science and Technology Building	MUA	-	GCHP	2011
56	Wuhan University of Technology Building	MUA	-	GCHP	2011
57	Optics Valley Building	MUA	123574	GCHP	2011
58	Ao Shang Century City Court	MUA	300000	GCHP	2012

The distribution of different types of installed geothermal systems is presented in Fig. 12. It is shown that the GSHPs are particularly located in the main urban area which also has a very high density of residents. The groundwater resource GSHPs are mainly located along the riverside of the Yangtze River due to a very shallow groundwater table and good potentials of unconfined aquifers. Compared to the GWHP systems, the GCHP systems are distributed more decentrally. It is indicated that the efficiency of a groundwater system depends largely on the hydraulic conditions of its aquifers, as shown in Fig. 7.

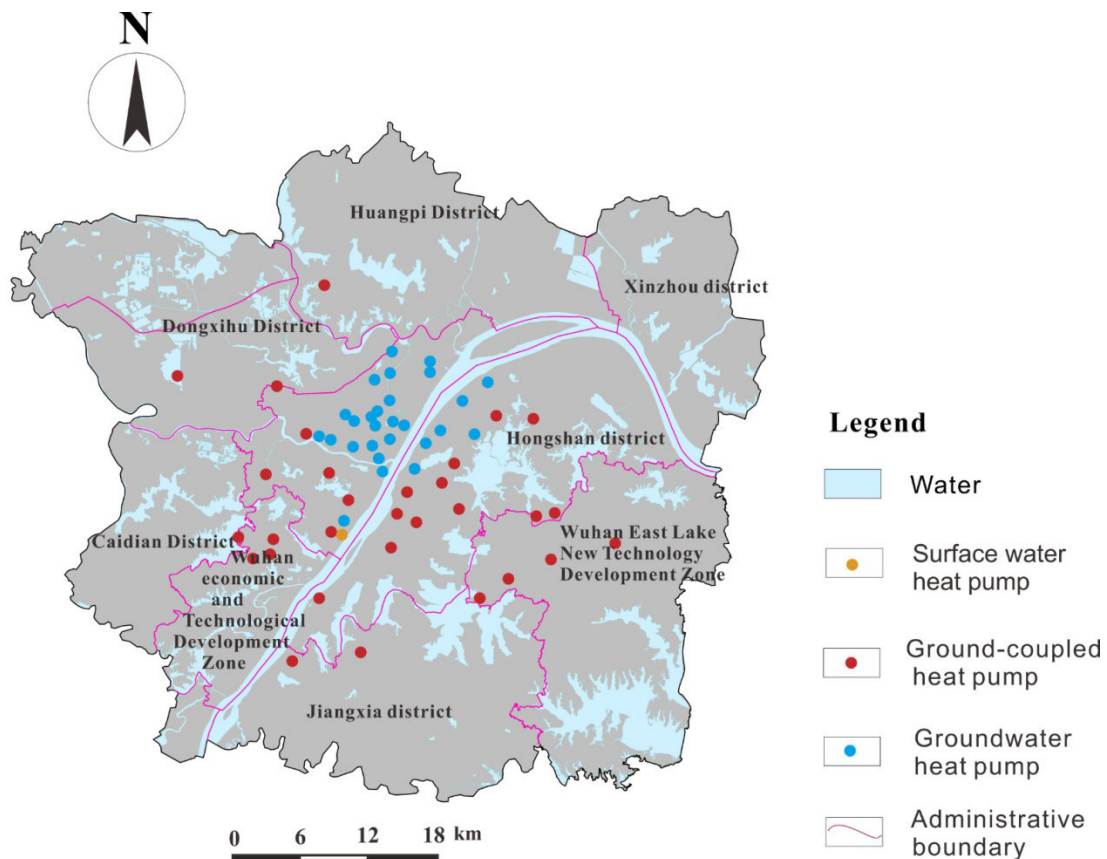


Fig. 12 Types and locations of the installed two types of ground source heat pump systems (GSHPs) in Wuhan city from 2001 to 2012

In order to examine the performance of the installed GSHPs, the system operation was measured. The coefficient of performance (COP) for both selected heat pumps and GSHP systems was determined. Due to Wuhan city is a cooling load dominated area, two types of GSHPs, the GWHP system and the GCHP system were investigated for operation in typical summer days. Fig. 13 shows the estimated daily performance of a GWHP system during the period from June till August in 2012. The obtained COP dataset shows a rather unstable performance for the system operation and the COP of the heat pump was relatively higher than the whole system.

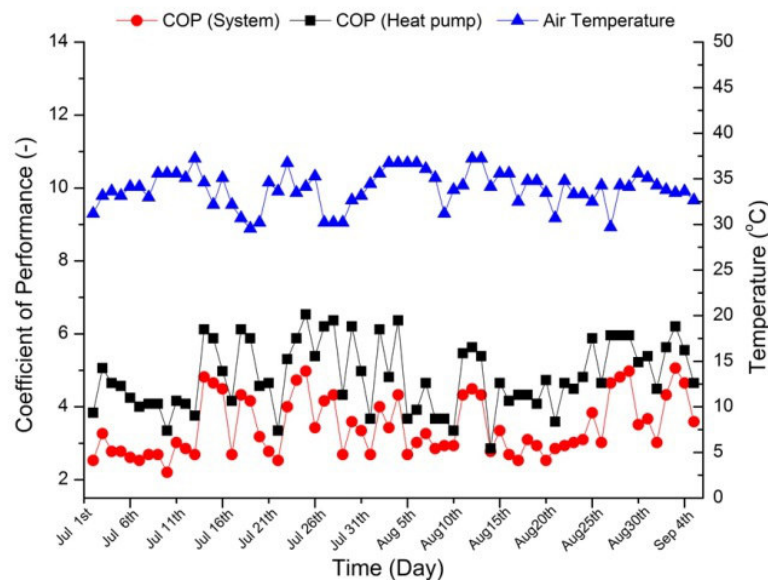


Fig.13 Performance of a groundwater heat pump system (GWHP) in typical summer days in Wuhan city (Xiangsheli Garden) in 2012

Fig. 14 shows the daily performance of a GCHP system during 1st, July till 31th, August in 2012. Similar to the GWHP system, the COP values of the GCHP system changed also drastically with time. Such a fluctuation can be caused by the timely high energy demand of the buildings. The GCHP systems use the geothermal energy from the surrounding soil and rocks by the coupled BHEs. The higher the energy leads to more drastic ground temperature changes, resulting in a lower performance of the whole system. Therefore it can be recognized that the GCHP systems have an

unstable performance.

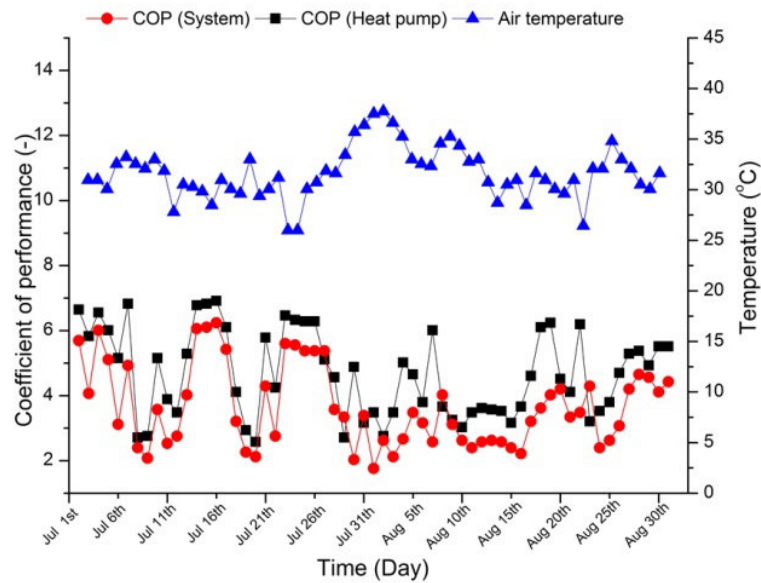


Fig. 14 Performance of a ground coupled heat pump system (GCHP) in typical summer days in Wuhan city (Qingjian Garden) in 2012

Furthermore, twenty-seven GSHPs including twenty one GCHPs and six GWHPs are selected for the evaluation of the Coefficient of Performance (COP) and the obtained results are presented in Table 9. These systems contain different types of buildings such as commercial buildings, hospital buildings, railway stations and residential buildings. The measurements were implemented for the GSHPs operation in summer since Wuhan city is a typical cooling load dominated area [41]. It can be observed that the heat pump operates with a higher performance than the whole system. For GCHPs, the average COP is measured to be 3.47 for the heat pumps and 3.20 for the systems in heating mode, 5.30 and 4.16 when the systems work in cooling mode. The COP for the GWHP is determined to be 3.64 for the heat pump and 3.04 for the system in winter, 4.66 and 4.24 in summer. Compared to the GWHP systems, GCHP works with slightly higher performance. This higher thermal efficiency of GCHP could be caused by the relatively stable ground temperature for such a type of geothermal system. As it is shown in Fig. 10, the ground temperature remains almost constant below a depth of 20 m. On the other hand, the GWHPs use the groundwater generally in a relatively shallow depth, in which the temperature fluctuates often with the different seasons. Therefore, the GCHP systems exhibit a higher efficiency than

the GWHPs.

Table 9 The estimated average coefficient of performance (COP) of the installed GCHPs and GWHPs in Wuhan city

System type	COP (heat pump)		COP (system)	
	Heating	Cooling	Heating	Cooling
GCHP	3.47	5.30	3.20	4.16
GWHP	3.64	4.66	3.04	4.24

5. Conclusions

The techno-economic feasibility of shallow geothermal systems depends strongly on the site conditions, i.e. geological properties and hydro-geological conditions. In this paper, the evaluation of the shallow geothermal potential in the urban area of Wuhan city was carried out with focus on three types of GSHPs. The climate was first analyzed with considering air temperature, wind and humidity. These data will be useful for characterizing the seasonal distribution of the thermal load for the local buildings. Then, the geological and hydro-geological conditions including stratigraphic sequence and lithology were investigated. Shallow geothermal resources were assessed with corresponding to different types of GSHP systems. Finally, the operation performance of the installed GSHP systems was examined. According to the geothermal investigations, the following conclusions can be drawn:

- Surface water geothermal potential: Wuhan city has a great potential of surface water resources for a SWHP installation. There are two main types of surface water systems, rivers and lakes. In the study area, there are 33 lakes and few rivers, in which Yangtze and Han Rivers are the main river systems. It shall be assumed that numerous of these GSHPs can be installed within such a type of resource. The useable energy source for SWHP installation capacity with lake and river systems is then estimated.
- Groundwater geothermal potential: The estimation of the groundwater resource for a GWHP installation is conducted by considering the unconfined aquifers. In order to provide exact data to guide practical installation of GSHPs, pumping rate of wells in the aquifers were estimated. In the urban area of Wuhan city, the unconfined aquifers in the Quaternary layers are distributed along the rivers which are considered to have a great potential for GWHPs due to the very high

pumping recharging rates of wells. The shallow geothermal potential for GWHP installation is mapped with three different categories, with highest potential area varies from 233 to 291 kW, followed by the second highly explorable geothermal potential ranges between 116 and 145 kW. The lowest explorable geothermal potential for GWHP is estimated mainly with the unconfined aquifers with a thickness of 5-20 m, which vary between 3 and 20 kW

- Ground soil/rock geothermal potential: The geothermal resource of the ground was assessed for the closed-loop GCHP installation. The thermal properties of the geological materials were first determined. It is shown that the thermal conductivity of the geological materials changes with the different materials. The rock exhibits generally higher thermal conductivities than the soil. Furthermore, the temperature distribution is measured within 120 m depth of the ground and a contour line map was created as a reference for the shallow geothermal exploration in the study area. Based on the ground thermal conditions investigations, thermal potential for GCHP installation is then estimated with seasonal energy and annual net energy exploration. Furthermore, thermal exchange rates of typical configured borehole heat exchangers were tested and the results show that heat transfer rates vary between 45.55 W/m to 66.80 W/m with different geometric configurations and ground conditions.
- Performance of the installed GSHP systems: The distribution and performance for different types of the GCHPs installed between the years 2001 and 2012 were investigated. GWHP systems are mainly installed along the riverside of the Yangtze River and the GCHPs are more randomly distributed. It is indicated that the installation of groundwater resource systems depends largely on the groundwater conditions. Furthermore, the examination of the performance of the GSHPs shows that the COP of both GCHPs and GWHPs vary drastically with timely energy demand. Compared to GWHPs, GCHPs operated with a higher efficiency due to the more stable temperatures in the deeper underground than that of the shallow aquifers.

Acknowledgements

This work was financially supported by National Natural Science Foundation of China (NSFC) (authorized No. 41502238) and Fundamental Research Funds for the

References

- [1] H. X. Yang, P. Cui, Z. H. Fang Vertical-borehole ground-coupled heat pumps: A review of models and systems. *Applied Energy*, 87(1) (2010): 16-27.
- [2] J.W. Lund, D.H. Freeston, T.L. Boyd. Direct utilization of geothermal energy 2010 worldwide review. *Geothermics* 40(2011):159-80.
- [3] L. Pu, D. Qi, K. Li, H. Tan, Y. Li, Simulation study on the thermal performance of vertical U-tube heat exchangers for ground source heat pump system, *Appl. Therm. Eng.* 79 (2015) 202-213.
- [4] Omer AM. Ground-source heat pumps systems and applications. *Renewable and Sustainable Energy Reviews* 2006; 12: 344-371.
- [5] P. Blum, G. Campillo, T. Kölbl. Techno-economic and spatial analysis of vertical ground source heat pump systems in Germany. *Energy*. 36(2011): 3002–3011.
- [6] L. Zhang, Q. Zhang, G. Huang, Y. Dua, A p(t)-linear average method to estimate the thermal parameters of the borehole heat exchangers for in situ thermal response test, *Applied Energy*, 131(2014): 211–221.
- [7] Viola Somogyin, Viktor Sebestyén, Georgina Nagy. Scientific achievements and regulation of shallow geothermal systems in six European countries – A review. *Renewable and Sustainable Energy Reviews* 68(2017)934–952.
- [8] Bertermann D., Klug H., Morper-Busch L. A pan-European planning basis for estimating the very shallow geothermal energy potentials. *Renewable Energy* 2015; 75: 335-347.
- [9] Alessandro Casasso, Rajandrea Sethi. Assessment and mapping of the shallow geothermal potential in the province of Cuneo (Piedmont, NW Italy). *Renewable Energy* 102 (2017) 306-315.
- [10] Jialing Zhu, Kaiyong Hu, Xinli Lu, Xiaoxue Huang, Ketao Liu, Xiujie Wu. A review of geothermal energy resources, development, and applications in China: Current status and prospects. *Energy* 93 (2015) 466-483.
- [11] Jiang J. *China's energy policy 2012*. Beijing, China: Information Office of the State Council, PRC; 2012.
- [12] Long H, Zhu Q, Tian P, Hu W. Technologies and applications of geophysical exploration in deep geothermal resources in China. In: *World Geothermal Congress 2015*; 2015. Melbourne, Australia.

- [13] MLR. Geologic exploration standard of geothermal resources. Beijing, China: Standards Press of China; 1989. p. 29.
- [14] Zhao X-g, Wan G. Current situation and prospect of China's geothermal resources. *Renew Sustain Energy Rev* 2014; 32: 651-61.
- [15] Wang G, Li K, Wen D, Lin W, Lin L, Liu Z, et al. Assessment of geothermal resources in China. In: *Thirty-Eighth Workshop on Geothermal Reservoir Engineering*. Stanford, California: Stanford University; 2013.
- [16] J.D. Spitler, X. Liu, S.J. Rees, C. Yavuzturk. Simulation and Optimization of Ground Source Heat Pump Systems. 8th International Energy Agency Heat Pump Conference. Las Vegas. May 30-June 2 (2005).
- [17] G. Florides, S. Kalogirou. Ground heat exchangers-a review of systems, models and applications. *Renew Energy* 32(2007): 2461-78.
- [18] Xiaojiang Ye, Fei Chen, Zhijian Hou. The effect of temperature on thermal sensation: a case study in Wuhan city, China. 9th International Symposium on Heating, Ventilation and Air Conditioning (ISHVAC) and the 3rd International Conference on Building Energy and Environment (COBEE). *Procedia Engineering* 121 (2015) 2149 – 2156
- [19] Ying Xiong, Jiabin Zhou, James J. Schauer, Wenyang Yu, Yan Hu. Seasonal and spatial differences in source contributions to PM_{2.5} in Wuhan, China. *Science of the Total Environment* 577 (2017) 155-165.
- [20] The 13th Five-Year Plan for Energy Development of the People's Republic of China, National Energy Administration, P.R. China, 2016.
- [21] Congjun Qin. A Study on the response of Wuhan climate under the background of global climate. Master thesis, College of Urban and environmental sciences, Central China Normal University, Wuhan, China, 2009.
- [22] Kaiser D P. Decreasing cloudiness over China: An updated analysis examining additional variables. *Geophysical Research Letters*, 2000, 27(15): 2193-2196.
- [23] Yang Yuwen , Ao Chenxia , Xiong Zengqiang. Wuhan Geology and Urban Geological Problems. *Urban Geotechnical Investigation & Surveying* 6(2015): 147-153.
- [24] Li Guosheng , Zhang Zhicheng , Meng Heiliang , Xu Hua. Wuhan Regional Geology and Stability. *Urban Geotechnical Investigation & Surveying* , 1(2017):164-168.

-
- [25] Wenfeng Wang, Anne Wairimu Ndungu, Zhen Li, Jun Wang. Microplastics pollution in inland freshwaters of China: A case study in urban surface waters of Wuhan, China. *Science of the Total Environment* 575 (2017) 1369-1374.
- [26] Wuhan Water Authority. Records of Lakes in Wuhan. Changjiang Publishing Media and Hubei Fine Arts Publishing House, Wuhan, 2015.
- [27] VDI-4640. Thermische Nutzung des Untergrundes: Grundlagen, Genehmigungen, Umweltaspekte (Thermal use of the underground: Fundamentals, approvals, environmental aspects), Part 1, Duesseldorf, Germany, 2000.
- [28] VDI-4640/2, Verein Deutscher Ingenieure, Blatt 2: Thermische Nutzung des Untergrundes - Erdgekoppelte Wärmepumpenanlagen [Part 2: Thermal use of the underground—ground source heat pump systems], 2001.
- [29] C.E. Jacob, Effective radius of drawdown test to determine artesian well, in: *Proceeding of the American Society of Civil Engineers, ASCE*, 1946, pp. 629-646.
- [30] B.D.R. Misstear, S. Beeson, Using operational data to estimate the reliable yields of water-supply wells, *Hydrogeol. J.* 8 (2) (2000) 177-187.
- [31] W.C. Walton, *Selected Analytical Methods for Well and Aquifer Evaluation*, Illinois State Water Survey, 1962.
- [32] B. Usowicz, J. Lipiec, J.B. Usowicz. Thermal conductivity in relation to porosity and hardness of terrestrial porous media. *Planet Space Sci* 56(2008): 438-47.
- [33] P. Münkkel. Untersuchung der thermischen Leitfähigkeit an Bohrkernen für die Eignung der flachen Geothermie. Bachelor-Thesis, Friedrich-Alexander-Universität Erlangen-Nürnberg, Erlangen, Germany. [unpublished] (2012).
- [34] A. Zarrella, G. Emmi, R. Zecchin, M. De Carli. An appropriate use of the thermal response test for the design of energy foundation piles with U-tube circuits. *Energy and Buildings* 134 (2017): 259–270.
- [35] Yang Zhang , Chen Yiyun, Ding Qing, Ping Jiang. Study on Urban Heat Island Effect Based on Normalized Difference Vegetated Index: A Case Study of Wuhan City. *Procedia Environmental Sciences* 13 (2012) 574 – 581.
- [36] C. Zhang, Z. Guo, Y. Liu, X. Cong, D. Peng. A review on thermal response test of GCHP systems. *Renew Sustain Energy Rev* 40 (2014):851-867.
- [37] N.H. Abu-Hamdeh, A.I. Khdair, R.C. Reeder. A comparison of two methods used to evaluate thermal conductivity for some soils. *Int J Heat Mass Transf* 44(2001): 1073-8.
- [38] H. Esen, M. Inalli. In-situ thermal response test for ground source heat pump

- system in Elazığ, Turkey. *Energy and Buildings* 41(2009): 395-401.
- [39] Luo J, Rohn J., Bayer M, Priess A, Xiang W. Thermal performance and economic evaluation of double U-tube borehole heat exchanger with three different borehole diameters. *Energy and Buildings* 67 (2013) 217–224.
- [40] P. Eskilson. Thermal analysis of heat extraction boreholes. Ph.D. Thesis. Sweden: University of Lund; 1987.
- [41] Yang Jing, Xu Linghong, Hu Pingfang, Zhu Na, Chen Xuepeng, Study on intermittent operation strategies of a hybrid ground-source heat pump system with double-cooling towers for hotel buildings, *Energy and Buildings* 2014; 76: 506-512.